ELSEVIER

International Journal of Solids and Structures 41 (2004) 1005–1019

INTERNATIONAL JOURNAL OF SOLIDS and STRUCTURES

www.elsevier.com/locate/ijsolstr

Structural and control optimization for maximum thermal buckling and minimum dynamic response of composite laminated plates

M.E. Fares, Y.G. Youssif, M.A. Hafiz *

Department of Mathematics, Faculty of Science, Mansoura University, Mansoura 35516, Egypt

Received 5 March 2003; received in revised form 23 September 2003

Abstract

A multiobjective optimization problem is presented to determine the optimal layer thickness and optimal closed loop control function for a symmetric cross-ply laminate subjected to thermomechanical loadings. The optimization procedure aims to maximize the critical combination of the applied edges load and temperature levels and to minimize the laminate dynamic response subject to constraints on the thickness and control energy. The objective of the optimization problem is formulated based on a consistent first-order shear deformation theory without introducing a shear correction factor. The dynamic response is measured as the sum of the total elastic energy of the laminate and a penalty term involving a closed loop control force. Laipunov–Bellman theory is used to obtain solutions for the controlled deflections and optimal control force. The layer thickness is taken as a design variable, and is presented as a function of the number of layers. A numerical study is made for simply supported symmetric laminates with an odd number of layers to show the advantages of the present control optimization. The study indicates that the present control optimization is active with most laminates cases for all values of aspect ratio, number of layers, orthotropy ratio, thermal expansions ratio and thickness ratio.

Keywords: Structural control; Design optimization; Thermal buckling; Dynamic response; Composite laminated plates; Design variables; Laipunov–Bellman theory

1. Introduction

Temperature changes frequently represent a significant factor of failure of composite structures subjected to sever environmental loads. The thermal stresses accompanying the non-uniform unsteady heating cause thermal fatigue and considerable plastic strains leading to complete or progressive destruction of the composite structures. Furthermore, the repeated action of the thermal stresses in some composite laminated

* Corresponding author. Tel./fax: +57731418.

E-mail addresses: sinfac@mum.mans.edu.eg (M.E. Fares), sinfac@mum.mans.edu.eg (Y.G. Youssif), mahafiz@gawab.com, mhafiz@islamway.net (M.A. Hafiz).

0020-7683/$ - see front matter © 2003 Elsevier Ltd. All rights reserved.
doi:10.1016/j.ijsolstr.2003.09.047

plates and shells leads to debonding of layers, longitudinal cracks, as well as, a thermal buckling in composite thin walled members. However, composite materials offer advantages over conventional materials, and they are more thermally stable than metals. To take advantage of the full potential of composite materials, structural analysts and designers must have extremely accurate tools of the analysis and design methods at their disposal. Optimization control is considered as the most effective mean for improving the performance of these composite structures to serve some functions under certain conditions.

A series of publications has appeared and concerning the design optimization and vibration control of large space structures. Many studies treated the design optimization and structural control as separate issues (see e.g. O'Donoghue and Atluri, 1986; Turvey and Marshall, 1995; Rao, 1989; Yang and Soong, 1988; Adali, 1984). In other studies, integrated approaches for the simultaneous design and control optimization were presented using a unified formulation (see e.g. Adali and Nissen, 1987; Rao, 1988; Salama et al., 1988; Cha et al., 1988). Rao et al. (1988) presented a multiobjective optimization approach with constrained imposed on the relevant quantities for truss and beams structures. Mesquita and Kamat (1988) used sequential structural and control optimization procedure for a stiffened composite laminate to improve a control performance index taking the fiber orientations and stiffener areas as design variables. More recent studies on this subject are available in the literature (Adali and Duffy, 1990a,b; Adali et al., 1991, 1997; Sloss et al., 1992; Sadek et al., 1993; Lee et al., 1999; Muc and Krawiec, 2000; Fares et al., 2002a,b; Wang and Huang, 2002; Youssif et al., 2001).

One inherent feature of composite laminates is that the transverse shear modulus is lower than the in-plane moduli and, as a result, the influence of transverse shear deformations becomes significant as the plate thickness increases. So, the application of the classical plate theory (CPT) which neglects the transverse shear effects, to composite laminates could leads to as much as 40% or more errors in the optimum values of the design and control variables (see Fares et al., 2002a,b). However, there are few studies, which treated the optimization control problems for composite laminates based on shear deformation theories.

The current work deals with the design and control optimization of composite laminates subjected to varying temperature distributions and in-plane compressive loadings. The design and control objectives of the problem are to maximize the thermal buckling, and to minimize the dynamic response with minimum expenditure of control force. The design and control objectives are formulated based on a consistent first-order shear deformation theory. This theory accounts for Reissner–Mindlin's displacement assumptions and stresses consistent with the surface conditions on the top and lower laminate surfaces (see Fares and Zenkour, 1999). So, the rationale for the shear correction factors used in other first-order theories is obviated. The dynamic response is expressed as the sum of the total elastic energy of the laminate and a penalty term involving the control force. Comparative examples are given for cross-ply symmetric laminates subject to temperature distribution varying linearly through the thickness and varying sinusoidally with respect to the in-plane coordinates. Also, the laminate edges are simply supported and loaded with biaxial stresses. The thickness of layers is taken as design variable which is presented as a function of the number of layers. The effectiveness of the present optimization design and control approach is examined.

2. Theoretical formulation

Consider a fiber reinforced rectangular laminate of constant thickness h occupying the space $0 \leqslant x \leqslant a$; $0 \leqslant y \leqslant b$; $-h/2 \leqslant z \leqslant h/2$. The laminate is composed of N anisotropic layers stacking in cross-ply lamination scheme such that each layer possesses one plane of elastic symmetry parallel to its mid-plane. The laminate is subjected to an temperature distribution varying linearly through the thickness and varying arbitrarily with respect to the in plane coordinates x and y,

$$T(x,y,z) = T_0(x,y) + \frac{z}{h}T_1(x,y). \tag{1}$$

Further, the laminate edges are loaded with biaxial compressions P_1 and P_2 (see Fig. 1). A control force $q(x,y,t)$ distributed over the upper surface of the laminate is taken to damp the dynamic response with the following initial disturbances:

$$w(x,y,0) = A^*(x,y); \quad \dot{w}(x,y,0) = B^*(x,y). \tag{2}$$

In general, the material properties and the thermal expansion coefficients depend upon the temperature level T (see Noor et al., 1994). But, for moderate increase in temperature, material properties may be considered independent of temperature. Here, we confine the study to materials with temperature-independent elastic properties. In addition, the assumed temperature does not exceed the buckling temperature. Consequently, the present problem may be formulated within the framework of linear elasticity theory.

The present formulation is based on a consistent first-order shear deformation theory that includes Ressiner–Mindlin's displacement assumptions and stresses consistent with the surface conditions on the top and lower laminates surfaces. So, the rationales for the shear correction factors used in other first-order theories are obviated. The displacement field is of the form:

$$u_1 = u + z\psi, \quad u_2 = v + z\phi, \quad u_3 = w, \tag{3}$$

where (u_1,u_2,u_3) are the displacements along x, y and z directions, respectively, (u,v,w) are the displacements of a point on the mid-plane, and ψ and ϕ are the shear rotations due to bending. The infinitesimal strains associated with the displacements (3) are given by:

$$\begin{aligned} &\varepsilon_1 = \varepsilon_1^0 + z\psi_{,x}, \quad \varepsilon_2 = \varepsilon_2^0 + z\phi_{,y}, \quad \varepsilon_3 = 0, \quad \varepsilon_4 = w_{,y} + \phi, \quad \varepsilon_5 = w_{,x} + \psi, \quad \varepsilon_6 = \varepsilon_6^0 + z\varepsilon_6^1, \\ &\varepsilon_1^0 = u_{,x}, \quad \varepsilon_2^0 = v_{,y}, \quad \varepsilon_6^0 = v_{,x} + u_{,y}, \quad \varepsilon_1^1 = \psi_{,x}, \quad \varepsilon_2^1 = \phi_{,y}, \quad \varepsilon_6^1 = \phi_{,x} + \psi_{,y}, \end{aligned} \tag{4}$$

a comma denotes partial differentiation with respect to the subscript.

The governing equations of the laminate are given in the form (see Fares and Zenkour, 1999):

$$N_{1,x} + N_{6,y} = I_1^*\ddot{u} + I_2^*\ddot{\psi}, \quad N_{6,x} + N_{2,y} = I_1^*\ddot{v} + I_2^*\ddot{\phi}, \tag{5a}$$

$$Q_{1,x} + Q_{2,y} + q = I_1^*\ddot{w} + (N_1 w_{,x} + N_6 w_{,y})_{,x} + (N_6 w_{,x} + N_2 w_{,y})_{,y}, \tag{5b}$$

$$M_{1,x} + M_{6,y} - Q_1 = I_2^*\ddot{u} + I_3^*\ddot{\psi}, \quad M_{6,x} + M_{2,y} - Q_2 = I_2^*\ddot{v} + I_3^*\ddot{\phi}, \tag{5c}$$

where the superposed dot denotes differentiation with respect to time, the inertias I_n^* and the constitutive equations are given by:

$$I_n^* = \sum_{k=1}^{N} \int_{z_{k-1}}^{z_k} \rho^{(k)} z^{n-1}\,\mathrm{d}z, \quad (n = 1,2,3),$$

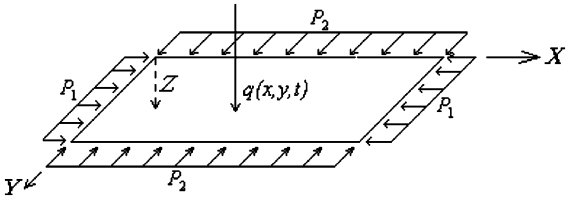

Fig. 1. Laminate subjected to in-plane compressive loadings and control force.

$$\begin{Bmatrix} N_1 \\ N_2 \\ N_6 \\ Q_2 \\ Q_1 \\ M_1 \\ M_2 \\ M_6 \end{Bmatrix} = \begin{bmatrix} A_{11} & A_{12} & A_{16} & 0 & 0 & B_{11} & B_{12} & B_{16} \\ A_{12} & A_{22} & A_{26} & 0 & 0 & B_{12} & B_{22} & B_{26} \\ A_{16} & A_{26} & A_{66} & 0 & 0 & B_{16} & B_{26} & B_{66} \\ 0 & 0 & 0 & A_{44} & A_{45} & 0 & 0 & 0 \\ 0 & 0 & 0 & A_{45} & A_{55} & 0 & 0 & 0 \\ B_{11} & B_{12} & B_{16} & 0 & 0 & D_{11} & D_{12} & D_{16} \\ B_{12} & B_{22} & B_{26} & 0 & 0 & D_{12} & D_{22} & D_{26} \\ B_{16} & B_{26} & B_{66} & 0 & 0 & D_{16} & D_{26} & D_{66} \end{bmatrix}^{-1} \begin{Bmatrix} \varepsilon_1^0 - N_1^{\mathrm{T}} \\ \varepsilon_2^0 - N_2^{\mathrm{T}} \\ \varepsilon_6^0 - N_6^{\mathrm{T}} \\ \varepsilon_4 \\ \varepsilon_5 \\ \varepsilon_1^1 - M_1^{\mathrm{T}} \\ \varepsilon_2^1 - M_2^{\mathrm{T}} \\ \varepsilon_6^1 - M_6^{\mathrm{T}} \end{Bmatrix}, \tag{6}$$

where $\rho^{(k)}$ is the material density of kth layer. The following definitions are used in the preceding equations:

$$(A_{ij}, B_{ij}, D_{ij}) = \sum_{k=1}^{N} \int_{z_{k-1}}^{z_k} C_{ij}^{(k)} \left(\frac{1}{h^2}, 12\frac{z,}{h^4} 144\frac{z^2}{h^6} \right) \mathrm{d}z \quad (i,j = 1,2,6), \tag{7a}$$

$$A_{ij} = \sum_{k=1}^{N} \int_{z_{k-1}}^{z_k} \frac{9}{4h^2} C_{ij}^{(k)} \left(1 - \frac{4z^2}{h^2} \right)^2 \mathrm{d}z \quad (i,j = 4,5), \tag{7b}$$

$$(N_i^{\mathrm{T}}, M_i^{\mathrm{T}}) = \sum_{k=1}^{N} \int_{z_{k-1}}^{z_k} \frac{\alpha_i^{(k)} T}{h^3} (h^2, 12z)\, \mathrm{d}z \quad (i = 1,2,6), \tag{7c}$$

where N_i^{T} and M_i^{T} are resultants and moments due to thermal loading, $\alpha_i^{(k)}$ are the coefficients of thermal expansion and $C_{ij}^{(k)}$ are the compliance elastic constants of the kth layer.

3. Optimal design/control problem

The design and control optimization objectives of the present study are to maximize the thermal buckling load and to minimize the vibrational response of the laminate (control objective) in a specified time $0 \leqslant t < \tau < \infty$ with the minimum possible expenditure of force $q(x,y,t)$. The total elastic energy of the laminated plate is taken as a measure of the dynamic response which is a function of displacements, its spatial derivatives and the velocity and is given by the following quadratic functional:

$$J_1(q,h_k) = \frac{1}{2} \int_0^{\infty} \int_0^{a} \int_0^{b} \int_{-\frac{h}{2}}^{\frac{h}{2}} [\varepsilon_i \sigma_i + \rho^{(k)} (\dot{u}_1^2 + \dot{u}_2^2 + \dot{u}_3^2)]\, \mathrm{d}z\, \mathrm{d}y\, \mathrm{d}x\, \mathrm{d}t, \quad (i = 1,2,\ldots,6), \tag{8}$$

where σ_i are the stresses due to the thermomechanical loadings.

Now, the present control problem aims to determine the minimum control function $q \in L^2$, where L^2 denotes the set of all bounded square integrable functions on the region $\{0 \leqslant x \leqslant a, 0 \leqslant y \leqslant b, 0 \leqslant t \leqslant \tau \leqslant \infty\}$, which, minimize the total elastic energy J_1 of the composite laminated plate. This conditional problem may be reduced to unconditional one by relating the total elastic energy J_1 with a penalty functional involving the control force $q(x,y,t)$ which may be taken as a measure of the energy used in the controlling process, then:

$$J_2 = J_1 + \xi_1 \int_0^{\tau} \int_0^{b} \int_0^{a} q^2(x,y,t)\, \mathrm{d}x\, \mathrm{d}y\, \mathrm{d}t. \tag{9}$$

Note that, the new functional J_2 is still quadratic and, hence, differentiable and positive definite on the domain of solution. This problem may be solved using Liapunov–Bellman theory (see Gabralyan, 1975) to determine the optimal control force q^0.

The design procedure aims to maximize the critical buckling temperature $T_c(h_k)$ and minimize the control objective function $J_2(q^0, h_k)$. Then, we can unified the critical buckling temperature $T_c(h_k)$ and the control objective $J_2(q^0, h_k)$ in a single expression of the form:

$$J_3(q^0, h_k) = J_2(q^0, h_k) + \xi_2/T_c(h_k), \tag{10}$$

where ξ_1 and ξ_2 are positive constant weighting factors. Then the optimal design aims to determine the optimal ply thickness h_k that minimize J_3.

4. Solution procedure

The solution of this problem can be performed in two parts (see Boley and Weiner, 1960). The first one is to determine the in-plane stresses N_1, N_2 and N_6 and the in-plane displacements u and v. The second part makes use of these results, to yield the displacements w, ψ and ϕ. For the present problem the solution will be constructed for simply supported symmetric cross-ply laminates which has the feature that:

$$A_{16} = A_{26} = A_{45} = 0, \quad B_{ij} = 0, \ (i, j = 1, 2, 6), \quad D_{16} = D_{26} = 0, \quad \alpha_6 = 0.$$

In this case, we can easily obtain from system of equations (6) the following constitutive equations:

$$\begin{bmatrix} \varepsilon_1^0 \\ \varepsilon_2^0 \\ \varepsilon_6^0 \end{bmatrix} = \begin{bmatrix} A_{11} & A_{12} & 0 \\ A_{12} & A_{22} & 0 \\ 0 & 0 & A_{66} \end{bmatrix} \begin{bmatrix} N_1 \\ N_2 \\ N_6 \end{bmatrix} + \begin{bmatrix} N_1^T \\ N_2^T \\ N_6^T \end{bmatrix}, \tag{11a}$$

$$\begin{bmatrix} \varepsilon_1^1 \\ \varepsilon_2^1 \\ \varepsilon_6^1 \end{bmatrix} = \begin{bmatrix} D_{11} & D_{12} & 0 \\ D_{12} & D_{22} & 0 \\ 0 & 0 & D_{66} \end{bmatrix} \begin{bmatrix} M_1 \\ M_2 \\ M_6 \end{bmatrix} + \begin{bmatrix} M_1^T \\ M_2^T \\ M_6^T \end{bmatrix}, \tag{11b}$$

$$[\varepsilon_4, \varepsilon_5] = [A_{44}Q_2, A_{55}Q_1]. \tag{11c}$$

The first step of solution is performed using the governing equations (5a) and the constitutive equations (11a). Eqs. (5a) are satisfied identically by introducing the Airy stress function $F(x, y)$,

$$N_1 = F_{,yy}, \quad N_2 = F_{,xx}, \quad N_6 = -F_{,xy}, \tag{12}$$

using expressions (11a) with the in-plane strain compatibility equation, namely (see Turvey and Marshall, 1995).

$$\frac{\partial^2 \varepsilon_1^0}{\partial y^2} + \frac{\partial^2 \varepsilon_2^0}{\partial x^2} - \frac{\partial^2 \varepsilon_6^0}{\partial x \partial y} = 0, \tag{13}$$

we get for the stress function the following fourth-order partial differentiable equation:

$$A_{11}F_{,yyyy} + A_{22}F_{,xxxx} + (A_{66} + 2A_{12})F_{,xxyy} + N_{1,yy}^T + N_{2,xx}^T = 0. \tag{14}$$

The boundary conditions at the laminate edges will be taken to stipulate that the edges of the plate remain straight, that is,

$$u(0, y) = 0, \quad v(x, 0) = 0, \quad u(a, y) = u_0, \quad v(x, b) = v_0, \tag{15}$$

where u_0 and v_0 are constants, consistently with the following conditions on the resultant forces on the ends:

$$\int_0^b N_1(0, y)\,\mathrm{d}y = \int_0^b N_1(a, y)\,\mathrm{d}y = bhP_1, \quad \int_0^a N_2(x, 0)\,\mathrm{d}x = \int_0^a N_2(x, b)\,\mathrm{d}x = ahP_2. \tag{16}$$

A solution of Eq. (14) that satisfies the conditions (16) may be obtained in the form:

$$F = \frac{1}{2}P_1 h y^2 + \frac{1}{2}P_2 h x^2 + c_1 N^{\mathrm{T}}_{1,yy} + c_2 N^{\mathrm{T}}_{2,xx}, \tag{17}$$

with the help of solution (17), Eqs (11a) and (12), we can determine the in-plane forces N_1, N_2, N_6 and the displacements u and v.

The second step of the solution consists in the determination of the deflection w and of the critical combination of the applied load and temperature levels. This is done with the aid of equations (5b), (5c), (11b) and (11c), with the following boundary conditions appropriate to simply supported edges:

$$\begin{aligned} &M_1 = w = \phi = 0, \quad \text{at } x = 0, a, \\ &M_2 = w = \psi = 0, \quad \text{at } y = 0, b. \end{aligned} \tag{18}$$

The exact solution of the above system of partial differential equations (5b) and (5c) under the boundary conditions (18), may be obtained by expressing the functions w, ψ and ϕ and the closed-loop control function q in the form:

$$(w, \psi, \phi, q) = \sum_{m,n} (W_{mn} XY, \Psi_{mn} X_x Y, \Phi_{mn} X Y_y, Q_{mn} XY), \tag{19}$$

where W_{mn}, Ψ_{mn}, Φ_{mn} and Q_{mn} are unknown functions of time, and the functions $X(x)$ and $Y(y)$ have the forms:

$$X(x) = \sin \mu_m x, \quad \mu_m = m\pi/a, \quad Y(y) = \sin \lambda_n y, \quad \lambda_n = n\pi/b.$$

Substituting expressions (11b), (11c) and (19) into Eqs (5b) and (5c), we obtain after some mathematical manipulations, the following time system of equations:

$$[\overline{R}]\{K\} + [L]\{\ddot{K}\} = \{f\}, \tag{20}$$

where $\{K\}$, $\{\ddot{K}\}$ and $\{f\}$ are the displacements, the inertia and the force vectors, respectively. The matrices $[\overline{R}]$ and $[L]$ are given in Appendix A.

The present problem is solved under the assumption that the buckling and vibration of laminate occur at different times during its service life (see Sloss et al., 1992). Then, the prebuckling response may be determined by solving Eq. (20) with the non-linear terms involving thermal stresses omitted. While, the critical buckling temperature rise T_c is found by solving the eigenvalue problem associated with equations (20) in which the control force and inertia terms are dropped. In this case, system (20) is reduced to a homogeneous linear algebraic system of three equations with three unknowns:

$$[\overline{R}]\{K\} = \{0\}. \tag{21}$$

5. Optimal control force

The optimal control force q^0 and controlled deflection W^0_{mn} corresponding to the prebuckling response may be found from the system of equations (20), with the non-linear terms including the thermal stresses and the in-plane inertia terms omitted. Then, an equation of the time-dependent functions W_{mn} and Q_{mn} may be obtained in the form:

$$\begin{aligned} &\ddot{w}_{mn} + \omega^2_{mn} W_{mn} = Q_{mn}/I^*_1, \\ &\omega^2_{mn} = \frac{1}{e^2_0 I^*_1 I_1}(e_3 \Psi_3 + e_4 \Phi_3 + e_0 W_3). \end{aligned} \tag{22}$$

Also, using expressions (11) and (19) with (9), to get the cost functional J_2 in the form:

$$J_2 = \sum_{m,n} \int_0^\infty (\delta_1 W_{mn}^2 + \delta_2 \dot{W}_{mn}^2 + \delta_3 Q_{mn}^2)\,\mathrm{d}t = \sum_{m,n} J_{mn}, \tag{23}$$

where the quantities I_1, e_i and δ_i are given in Appendix A. Since the system of equations (20) is separable, hence the functional (23) depends only on the variables found in (m,n)th equations of the system. With the aid of this condition, the problem is reduced to a problem of analytical design of controllers (see Gabralyan, 1975), for every m, $n = 1, 2, \ldots, \infty$.

Now the optimal control problem is to find a control function $q^0(t)$ that satisfies the conditions:

$$J_2(q^0) \leqslant J_2(q), \quad \text{for all } q(t) \in L^2([0,\infty]),$$

that is:

$$\min_q J_2 = \min_q \sum_{m,n} J_{mn} = \sum_{m,n} \min_{Q_{mn} \in L^2} J_{mn}.$$

Hence, the minimization problem can be carried out independently for every modal equation. For such problem, Liapunov–Bellman theory (see Gabralyan, 1975) is considered as an effective approach to solve it. The necessary and sufficient conditions according to Liapunov–Bellman theory for minimizing the functional (23) is:

$$\min_{Q_{mn}} \left[\frac{\partial V_{mn}}{\partial W_{mn}} \dot{W}_{mn} + \frac{\partial V_{mn}}{\partial \dot{W}_{mn}} \ddot{w}_{mn} + \overline{J}_{mn} \right] = 0, \tag{24}$$

provided that the Liapunov function $V_{mn,}$

$$V_{mn} = A W_{mn}^2 + 2B W_{mn} \dot{W}_{mn} + C \dot{W}_{mn}^2, \tag{25}$$

is a positive definite, i.e. $A > 0$, $C > 0$ and $AC > B^2$, where $\overline{J}_{mn}$ is the integrand of (23). Using Eq. (24), we can obtain the optimal control function in the form:

$$Q_{mn}^0 = \frac{-1}{\delta_3 I_1^*} (B W_{mn} + C \dot{W}_{mn}), \tag{26}$$

then, substituting Eqs (22), (23), (25) and (26) into the condition (24), and equating the coefficients of W_{mn}^2, $\dot{W}_{mn}^2$ and $W_{mn}\ \dot{W}_{mn}$ by zero, we get a system of equations. The general solution of this system under the condition that the Liapunov function is a positive definite is given by:

$$B = -I_1^{*2} \left[\omega_{mn}^2 \delta_3 - \sqrt{\delta_3 \left(\omega_{mn}^4 \delta_3 + \frac{\delta_1}{I_1^{*2}} \right)} \right], \quad C = -I_1^* \sqrt{\delta_3 (2B + \delta_2)}, \tag{27}$$

using expressions (26) and (27) into Eq. (22), it takes the form:

$$\ddot{w}_{mn} + \alpha_{mn} \dot{w}_{mn} + \Omega_{mn}^2 W_{mn} = 0, \quad \alpha_{mn} = \frac{C}{\delta_3^2 I_1^{*4}}, \quad \Omega_{mn}^2 = \omega_{mn}^2 + \frac{B}{\delta_3 I_1^{*2}}. \tag{28}$$

The solution of Eq. (28) for which $2\Omega_{mn} > \alpha_{mn}$, is given by:

$$W_{mn}^0 = \mathrm{e}^{-\alpha_{mn} t/2} [\beta_{mn} \cos(\bar{\nu}_{mn} t) + \gamma_{mn} \sin(\bar{\nu}_{mn} t)], \quad \bar{\nu}_{mn}^2 = \Omega_{mn}^2 - \frac{1}{4} \alpha_{mn}^2, \tag{29}$$

where β_{mn} and γ_{mn} are unknown coefficients which may be obtained from the initial conditions (1) by expanding it in double Fourier series, then:

$$\gamma_{mn} = \frac{\alpha_{mn}\beta_{mn} + 2A^*_{mn}}{2\bar{v}_{mn}}, \quad (\beta_{mn}, A^*_{mn}) = \frac{4}{ab\omega^2_{mn}} \int_0^a \int_0^b (A^*, B^*) XY \, \mathrm{d}x \, \mathrm{d}y. \tag{30}$$

Insert the expressions (29) and (30) into Eqs (23) and (26) we can obtain the total elastic energy and the optimal control force.

6. Critical temperature and optimal design procedure

The critical combination of the applied edges loads and temperature levels, at which the buckling occurs, may be determined from the requirement for a non-zero solution of system (21). Thus, we must set the determinant $|\overline{R}|$ equal to zero, i.e.

$$|\overline{R}| = 0, \quad \text{or} \quad |R| - \lambda|U| - P|\overline{U}| = 0, \tag{31}$$

where the matrices $[U]$, $[\overline{U}]$ and $[R]$ are given in Appendix A, λ is the non-dimensional temperature parameter where $\lambda = \alpha_1 T_0 \times 10^2$, $T_1 = 10T_0$, and P is the non-dimensional edges load parameter, $P = 100P_1/E_2$, $P_1 = P_2$. For a given value of P less than the pure critical edges loads, the lowest value of λ with respect to mode numbers (m, n) represents the critical value of temperature rise T_c. Also, for a given value of λ less than the pure critical temperature rise, the lowest value of P with respect to mode numbers (m, n) represents the critical value of buckling load P_c, i.e.

$$T_c = \min_{m,n} \lambda, \quad P_c = \min_{m,n} P, \quad m, n \geqslant 1. \tag{32}$$

The aim of the design procedure is to maximize the critical buckling temperature T_c using the layer thickness h_k as a design variable. So, for the numerical purpose, we consider a general symmetric laminates with a stacking sequence (0°/90°/0°...) having an odd number N of layers with thicknesses: $(h_1, h_2, h_{3,}, \ldots / \ldots, h_3, h_2, h_1)$, $h_1 = h_3 = h_5 = \cdots, h_2 = h_4 = h_6 \cdots$ (see, Fig. 2).

In this case, we can formulate the layer thickness h_k as a function of number of layers N by introducing a thickness ratio η as follows:

$$h_k = \begin{cases} \eta h/2: & k = (1, 3, \ldots, N) \\ h[4 - \eta(N+1)]/(2N-2): & k = (2, 4, \ldots, N-1). \end{cases}$$

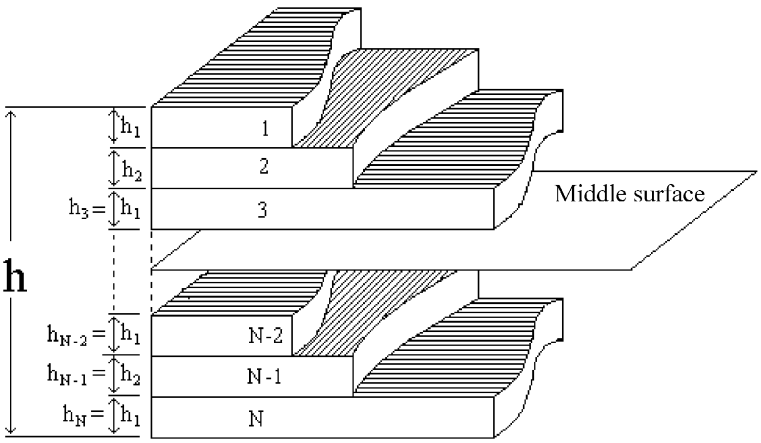

Fig. 2. Geometry and cross section of the symmetrically laminated cross-ply laminate.

Therefore, the optimum values η_{opt} of the thickness ratio are determine from the following conditions:

$$J^0(\eta_{opt}) = \min_{\eta} J_3(\eta), \quad 0 \leqslant \eta \leqslant 4/(1+N). \tag{33}$$

7. Numerical results and discussion

In this section, numerical results for the controlled deflections w^0, optimal force q^0 and the total elastic energy J_1 are presented when all layers are orthotropic. The engineering constants are introduced instead of the elastic constants from the relations:

$$C_{11} = \frac{1}{E_1}, \quad C_{22} = \frac{1}{E_2}, \quad C_{12} = -\frac{v_{12}}{E_1}, \quad C_{23} = -\frac{v_{23}}{E_2}, \quad C_{13} = -\frac{v_{13}}{E_1}, \quad C_{44} = \frac{1}{G_{23}},$$
$$C_{55} = \frac{1}{G_{13}}, \quad C_{66} = \frac{1}{G_{12}}, \tag{34}$$

where E_i are Young's moduli; v_{ij} are Poisson's ratios and G_{ij} are shear moduli. The initial conditions (2) are chosen in the form:

$$w(x,y,0) = 10^{-3}X(x)Y(y), \quad \dot{w}(x,y,0) = 0. \tag{35}$$

In all calculations, unless otherwise stated, the following parameters are used,

$$E_1/E_2 = 25, \quad G_{12}/E_2 = 0.5, \quad G_{23}/E_2 = 0.2, \quad v_{13} = v_{12}, \quad v_{12} = 0.25, \quad G_{13} = G_{12},$$
$$a/h = 15, \quad \alpha_2/\alpha_1 = 3, \quad \xi_1 = 0.1, \quad \xi_2 = 1, \quad t^* = t\sqrt{E_2}/\rho, \quad \bar{q} = 100q/E_2,$$
$$u_0 = v_0 = 0, \quad N = 3. \tag{36}$$

The numerical results for deflections and force functions are given at the midpoint $x = a/2$, $y = b/2$. Table 1 contains numerical results of the optimal thickness ratio η_{opt}, critical temperature level T_c^0 for laminates designed optimally over the thickness and critical temperature level T_c for laminates with equi-thickness layers. In this table, the variations of η_{opt}, T_c^0 and T_c are studied with respect to the edges load P, number of layers N and aspect ratio a/b. Note that, the optimal design procedure is more required for square like laminates which have low resistance to thermal buckling, than the long laminates ($a/b \geqslant 3$). Also when $P = 0$, the critical temperature level T_c^0 for optimally designed laminates is approximately four times its corresponding value for non-optimal ones. Further, the ratio between T_c^0 and T_c increases gradually with increasing the edges loads P_c. The postbuckling edges loads with respect to the non-optimal laminates ($P_c \geqslant 1$ in case I and $P_c \geqslant 2$ in case II) become prebuckling loads with respect to the optimal ones. So that, in all cases, the minimum values of T_c^0 for optimal laminates are greater than the maximum values of T_c for non-optimal ones. Then, the present design procedure raises the critical combination level of the applied load and temperature. Further, we observe that the edges load P has a weak effect on the optimal thickness ratio η_{opt}, where η_{opt} increases very slowly with increasing P_c. While, the effect of the aspect ratio a/b on η_{opt} is more considerable, particularly, for long laminates so that for laminates with $1 < a/b < 2$, the optimal thickness ratio η_{opt} takes values between 0.92 and 0.86, while, for laminates with $2 < a/b < 3$, the ratio η_{opt} takes values between 0.86 and 0 ($P_c \leqslant 2$). Here, the optimal laminate corresponding to the case $\eta_{opt} = 0$ represents a single layer plate with fiber orientation angle 90°.

The improved critical values of temperature and edges load at which buckling occur for different values of a/b and N are given in Table 2 for three buckling cases, where P_{c0}^0 corresponds to a critical pure edges loads ($T = 0$), T_{c0}^0 represents a critical pure thermal load ($P = 0$), and (P_c^0, T_c^0) corresponds to the general case in which both heat and edges loads are applied. These results may be seen to fit accurately the formula:

Table 1
The critical temperature T_c for some cases of load P_c and a/b $\alpha_2/\alpha_1 = 3$, – means any temperature

P_c	$N = 3$			$N = 5$			$N = 7$		
	η_{opt}	T_c^0	T_c	η_{opt}	T_c^0	T_c	η_{opt}	T_c^0	T_c
Case I. a/b = 1									
0	0.92	6.102	1.525	0.66	5.694	1.395	0.5	6.003	1.365
0.5	0.93	5.387	0.649	0.66	4.993	0.514	0.5	5.305	0.482
1	0.93	4.673	–	0.66	4.292	–	0.5	4.606	–
2	0.94	3.248	–	0.66	2.891	–	0.5	3.209	–
3	0.96	1.829	–	0.66	1.489	–	0.5	1.812	–
Case II. a/b = 2									
0	0.86	5.248	3.717	0.66	4.808	3.664	0.5	4.921	3.653
0.5	0.87	4.386	2.646	0.66	4.013	2.589	0.5	4.132	2.577
1	0.88	3.529	1.576	0.66	3.217	1.514	0.5	3.342	1.500
2	0.91	1.837	–	0.66	1.625	–	0.5	1.762	–
3	0.97	0.186	–	0.66	0.034	–	0.5	0.183	–
Case III. a/b = 3									
0	0	11.13	10.72	0	11.13	10.73	0	11.13	10.74
0.5	0	9.301	8.976	0	9.301	8.976	0	9.301	8.977
1	0	7.468	7.229	0	7.468	7.213	0	7.468	7.216
2	0.78	4.232	3.736	0.66	3.803	3.701	0	3.803	3.696
3	0.85	1.725	0.242	0.66	1.394	0.188	0.5	1.450	0.175

Table 2
The critical values of edges load P and temperature T_c for three cases of a/b

Load	$a/b = 1$			$a/b = 2$			$a/b = 3$		
	$N = 3$	$N = 5$	$N = 7$	$N = 3$	$N = 5$	$N = 7$	$N = 3$	$N = 5$	$N = 7$
$T = 0$, $P_{c0}^0 =$	4.297	4.063	4.297	3.119	3.021	3.116	3.778	3.720	3.763
$P = 0$, $T_c^0 =$	6.102	5.694	6.003	5.248	4.808	4.921	11.13	11.13	11.13
$P = \frac{1}{2}$, $T_c^0 =$	5.387	4.993	5.305	4.386	4.013	4.132	9.301	9.301	9.301
$P = 1$, $T_c^0 =$	4.673	4.292	4.606	3.529	3.217	3.342	7.468	7.468	7.468
$P = 2$, $T_c^0 =$	3.248	2.891	3.209	1.837	1.625	1.762	4.232	3.803	3.803
$P = 3$, $T_c^0 =$	1.829	1.489	1.812	0.186	0.034	0.183	1.725	1.394	1.394

$$\frac{T_c^0}{T_{c0}^0} + \frac{P_c^0}{P_{c0}^0} = 1 \tag{37}$$

for all aspect ratios, number of layers and all combinations of heat and edges loadings. Fig. 3 shows obviously this fact which agrees with the results obtained in other studies (see Boley and Weiner, 1960; Turvey and Marshall, 1995). For design process, Eq. (37) may be helpful in determination of buckling loads of heated and loaded laminates. Fig. 4 shows the variation of T_c with respect to P_c for optimal and non-optimal laminates. This figure reveals that the design procedure raises significantly the level of the critical temperature for all values of edges loads.

The effects of side-to-thickness ratio a/h and thermal expansions ratio α_2/α_1 on the optimization process are displayed in Fig. 5 which shows that the optimal design over the thickness is needed for all values of a/h and α_2/α_1. Also, the optimal design is very active for moderately thick laminates with low values of α_2/α_1, while it is inactive for thin laminates with high values of α_2/α_1. This is may be explained by the fact that thin

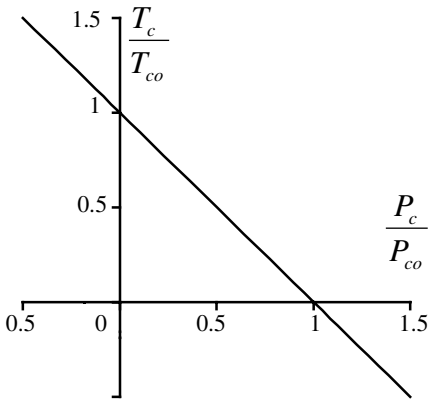

Fig. 3. Interaction of temperature level and applied stress for buckling of the laminates.

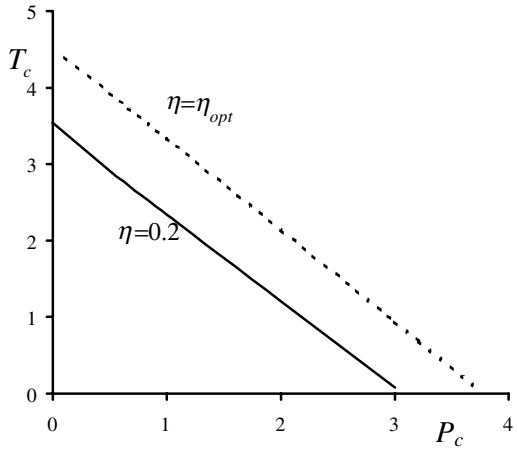

Fig. 4. T_c-curves plotted against P, (- - -) for $\eta = \eta_{opt}$, (—) for $h_k = 2h/N$, $a/b = 3$ and $\alpha_2/\alpha_1 = 10$.

laminate has a very low resistance to thermal buckling. In addition, the large difference between the thermal expansion coefficients α_1 and α_2 in cross-ply laminates makes that the layers under the thermal load exhibit various elastic behaviors causing decrease in the laminate resistance to thermal buckling.

Fig. 6 contains T_c-curves plotted against the side-to-thickness ratio a/h for laminates with three, five and seven layers. It is worth noting that the optimization over the thickness makes always to reduce the number of layers. This is due to the fact that the laminate with few symmetric layers is more homogeneous and resists the thermal buckling.

Fig. 7 includes curves of the controlled elastic energy $\overline{J}_3(= 100J_1/E_2)$ plotted against the orthotropy ratio E_1/E_2 and temperature levels $(10^3\alpha_0 T_0)$. These curves indicate that beside the control force, the optimization over the thickness considerably reduces the energy level of the laminate as compared to a non-optimal one. In addition, the elastic energy still is reduced by virtue of the optimization with respect to the design variable only without active control (see Fig. 8). Then the design optimization by itself can reduce the dynamic response. Also, of course, as the temperature increase, the elastic energy significantly increase,

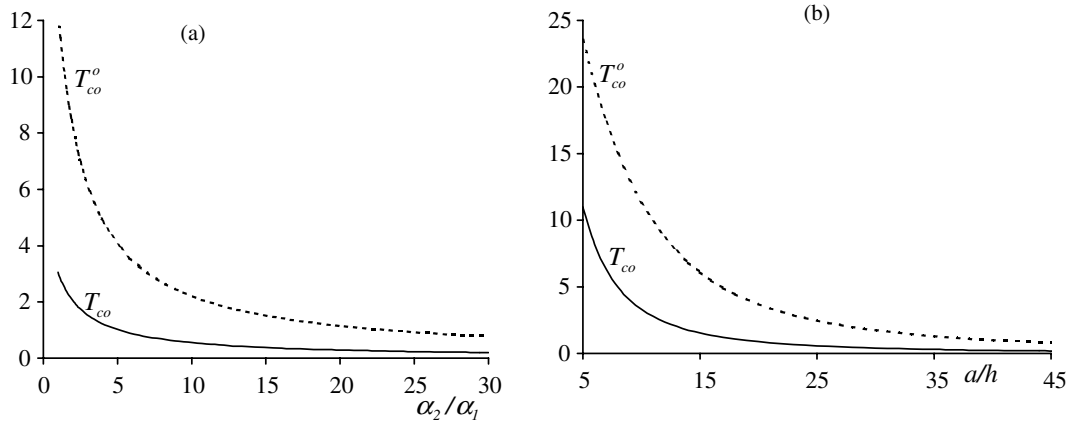

Fig. 5. Curves of T_{c0}^{0} and T_{c0} plotted against α_2/α_1 and a/h, $P = 0$ and $a/b = 1$, (- - -) for optimal laminates, (—) for equal thickness.

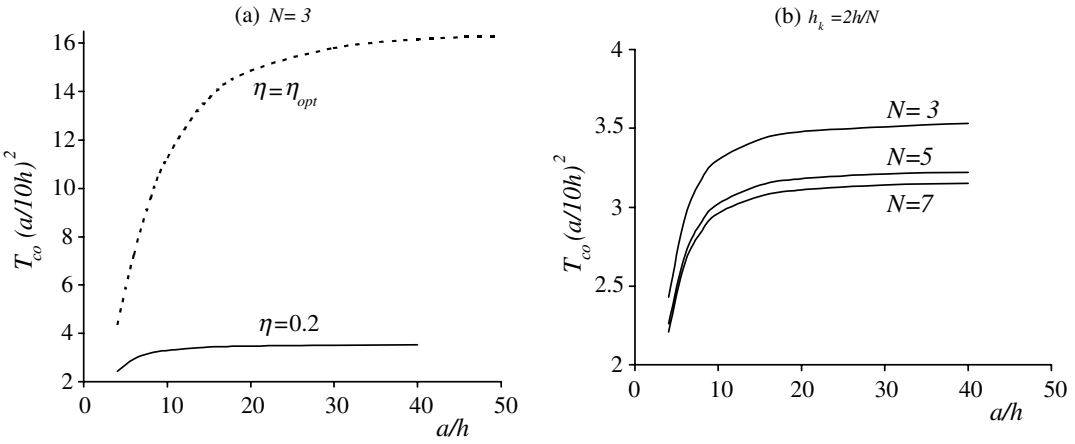

Fig. 6. Curves of T_c plotted against a/h, $P = 0$ and $a/b = 1$.

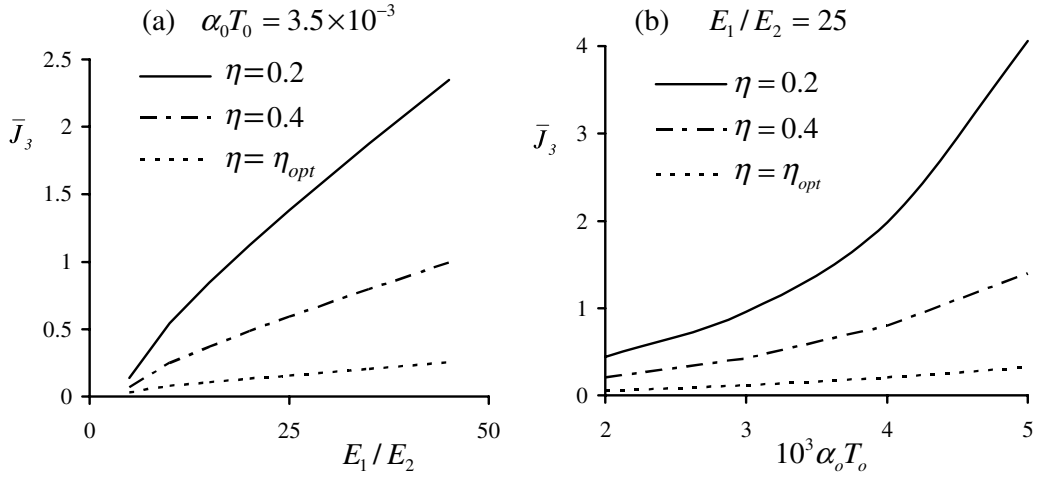

Fig. 7. Curves of $\bar{J}_3$ plotted against E_1/E_2 in (a) and against $10^3\alpha_0 T_0$ in (b) for $P/E_0 = 3 \times 10^{-3}$.

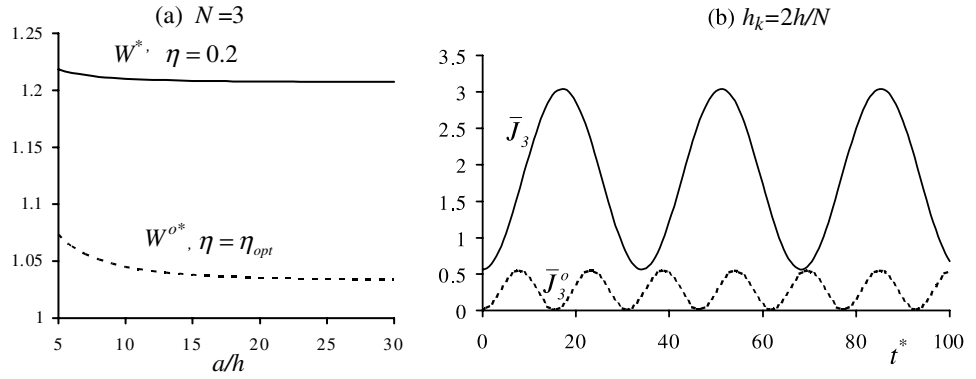

Fig. 8. Comparison of center deflections $W^* = 10hW/(\alpha_1 T_1 a^2)$ in (a) and the elastic energy $\bar{J}_3$ in (b) of (0°/90°/0°) symmetric laminates, $q = 0$, $T_0 = 0$.

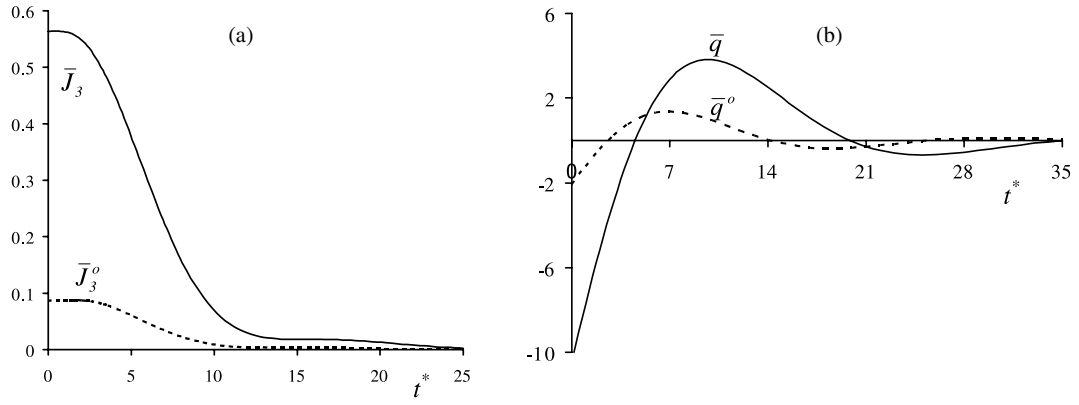

Fig. 9. Curves of the elastic energy $\bar{J}_3$ and the optimal control force q^0 plotted against t^* for square laminate with $a/h = 15$, $P = T = 0$.

but, the optimal design procedure reduces and damps this behavior causing that the energy slowly increases with the increase of the temperature level. The laminates exhibit similar behavior with increasing the orthotropy ratio. This is may due to the fact that the design optimization makes the laminate is more stiffer in bending and has smaller deflections when compared to the non-optimal one (see Fig. 7(a)). The behavior of the controlled energy $\bar{J}_3$ and control force $\bar{q}^0 (= 100q^0/E_2)$ with time t^* is studied in Fig. 9. Note that the optimization control not only reduces the elastic energy, but also, reduces the expenditure of control energy and the time of damping process.

8. Conclusion

The optimal layer thickness and optimal closed loop control function are determined in a multiobjective formulation of the design and control problem for a symmetric cross-ply laminate with simply supported edges. The objectives of the present study are the maximization of the critical combination of the applied edges loads and temperature levels and the minimization of the laminate dynamic response. The design and control objectives are formulated based on a consistent first-order shear deformation theory without introducing a shear correction factor. Numerical results are presented to show the advantages of the present

optimization control procedure. The numerical study indicates that the present control optimization is very active for moderately thick laminates and square like ones, particularly for laminates with low thermal expansions ratio α_2/α_1 and high, orthotropy ratio E_1/E_2. For these laminates, the control optimization is considerably reduces their dynamic response, but, it is less active in maximizing their thermal buckling. The design procedure without any control force reduces considerably the dynamic response of the laminate so that it limits the increase in laminate energy due to the increase in the temperature. Moreover, the present optimization approach not only maximizes the thermal buckling and minimizes the dynamic response, but also, it reduces the used control force and time of the damping process.

Appendix A

The coefficients e_i and δ_i at $T_0 = 0$ are:

$$\delta_1 = \frac{1}{2e_0^2}[I_{22}(e_3+e_4)^2/D_{66} + I_{16}(e_0+e_4)^2/A_{44} + I_{10}(e_3+e_0)^2/A_{55} + (e_4^2 D_{11} I_{23} - 2e_3 e_4 D_{12} I_7 + e_3^2 D_{22} I_8)/\overline{D}],$$

$$\delta_2 = (I_1^* I_1 + I_{10} I_3^* e_3^2/e_0^2)/2,$$

$$e_0 = (\Psi_4 \Phi_5 - \Psi_5 \Phi_4), \quad e_3 = W_5 \Phi_4 - W_4 \Phi_5, \quad e_4 = \Psi_5 W_4 - \Psi_4 W_5,$$

$$[\overline{R}] = \begin{bmatrix} \Psi_3 & \Phi_3 & W_3 - \lambda\gamma \\ \Psi_4 & \Phi_4 & W_4 \\ \Psi_5 & \Phi_5 & W_5 \end{bmatrix}, \quad [R] = \begin{bmatrix} \Psi_3 & \Phi_3 & W_3 \\ \Psi_4 & \Phi_4 & W_4 \\ \Psi_5 & \Phi_5 & W_5 \end{bmatrix},$$

$$[U] = \begin{bmatrix} \Psi_3 & \Phi_3 & \gamma \\ \Psi_4 & \Phi_4 & 0 \\ \Psi_5 & \Phi_5 & 0 \end{bmatrix}, \quad [\overline{U}] = \begin{bmatrix} \Psi_3 & \Phi_3 & \bar{\gamma} \\ \Psi_4 & \Phi_4 & 0 \\ \Psi_5 & \Phi_5 & 0 \end{bmatrix},$$

$$W_3 = I_5/A_{55} + I_6/A_{44}, \quad \Psi_3 = I_5/A_{55}, \quad \Phi_3 = I_6/A_{44},$$

$$W_4 = I_{10}\overline{D}/A_{55}, \quad \gamma_4 = I_{10}(D_{12} m_2^{\mathrm{T}} - D_{22} m_1^{\mathrm{T}}), \quad \Psi_4 = -I_{12} D_{22} + I_{10}\overline{D}/A_{55} - I_{14}\overline{D}/D_{66},$$

$$\Phi_4 = I_{14}(D_{12} - \overline{D}/D_{66}), \quad \gamma_5 = I_{16}(D_{12} m_1^{\mathrm{T}} - D_{11} m_2^{\mathrm{T}}), \quad W_5 = I_{16}\overline{D}/A_{44}, \quad \Psi_5 = I_{18}\overline{D}/A_{44},$$

$$\gamma = -I_{10}\mu_m^2 \lambda_n^2 (a_1 n_1^{\mathrm{T}} \lambda_n^2 + a_2 n_2^{\mathrm{T}} \mu_m^2), \quad \bar{\gamma} = 10^{-2} h E_1 (I_5 + I_6), \quad \overline{D} = (D_{11} D_{22} - D_{12}^2),$$

$$\Phi_5 = I_{16}\overline{D}/A_{44} - I_{18}\overline{D}/D_{66} - D_{11} I_{20}, \quad L_{33} = I_1 I_1^*, \quad L_{ij} = 0, (i,j = 4,5), \quad \{f\} = [q, \gamma_4, \gamma_5]^{\mathrm{T}},$$

where

$$(n_i^{\mathrm{T}}, m_i^{\mathrm{T}}) = \frac{1}{h\alpha_1 \times 10^2} \sum_{k=1}^{N} \int_{z_{k-1}}^{z_k} (\alpha_j, \alpha_j z^2 h^3/120)_k \, \mathrm{d}z, \quad (i,j = 1,2,6),$$

$$(I_1, I_5, I_6, I_7, I_8) = \int_0^a \int_0^b (XY, X_{,xx}Y, XY_{,yy}, X_{,xx}Y_{,yy}, XY_{,yy}) XY \, \mathrm{d}x \, \mathrm{d}y,$$

$$(I_{10}, I_{12}, I_{14}) = \int_0^a \int_0^b (X_{,x}Y, X_{,xxx}Y, X_{,x}Y_{,yy}) X_{,x}Y \, \mathrm{d}x \, \mathrm{d}y,$$

$$(I_{16}, I_{18}, I_{22}, I_{23}) = \int_0^a \int_0^b (X^2 Y_{,y}^2, X_{,xx} X Y_{,y}^2, X_{,x}^2 Y_{,y}^2, X_{,xx}^2 Y_{,y}^2)\,\mathrm{d}x\,\mathrm{d}y,$$

$$I_2 = I_3 = I_4 = I_9 = I_{11} = I_{13} = I_{15} = I_{17} = I_{19} = I_{20} = I_{21} = 0.$$

References

Adali, S., 1984. Design of shear-deformable antisymmetric angle-ply laminates to maximize the fundamental frequency and frequency separation. Composite Structures 2, 349–369.

Adali, S., Duffy, K.J., 1990a. Multicriteria thermoelastic design of antisymmetric angle-ply laminates. In: Eschenauer, H., Koski, J., Osyczka, A. (Eds.), Multicriteria Design Optimization. Springer-Verlag, Berlin, pp. 417–428.

Adali, S., Duffy, K.J., 1990b. Optimal design of antisymmetric hybrid laminates against thermal buckling. Journal of Thermal Stresses 13, 57–71.

Adali, S., Nissen, H., 1987. Optimization of antisymmetric angle-ply strip for maximum strength including hygrothermal effects. Journal of Mechanisms, Transmissions and Automation in Design 109, 192.

Adali, S., Sadek, I.S., Sloss, J.M., 1991. Simultaneous design/control optimization of symmetric cross-ply laminates of hybrid construction. Engineering Optimization 17, 123–140.

Adali, S., Richter, A., Verijenko, A.E., 1997. Minimum weight design of symmetric angle-ply laminates with incomplete information on initial imperfections. Journal of Applied Mechanics 64, 90–96.

Boley, B.A., Weiner, J.H., 1960. Theory of Thermal Stresses. Wiley, New York.

Cha, J.Z., Pitarressi, J.M., Soong, T.T., 1988. Optimal design procedures for active structures. Journal of Structural Engineering 114, 2710–2723.

Fares, M.E., Zenkour, A.M., 1999. Mixed variational formula for the thermal bending of laminated plates. Journal of Thermal Stresses 22, 347–366.

Fares, M.E., Youssif, Y.G., Alamir, A.E., 2002a. Optimal design and control of composite laminated plates with various boundary conditions using various plate theories. Composite Structures 56, 1–12.

Fares, M.E., Youssif, Y.G., Hafiz, M.A., 2002b. Optimization control of composite laminates for maximum thermal buckling and minimum vibrational response. Journal of Thermal Stresses 25 (11), 1047–1064.

Gabralyan, M.S., 1975. About stabilization of mechanical systems under continuous forces. YGU, Yervan, vol. 2, pp. 47–56.

Lee, Y.S., Lee, Y.W., Yang, M.S., Park, B.S., 1999. Optimal design of thick laminated composite plates for maximum thermal buckling load. Journal of Thermal Stresses 22, 259–273.

Mesquita, L., Kamat, M.P., 1988. Structural optimization for control of stiffened laminated composite structures. Journal of Sound and Vibration 116, 33–48.

Muc, A., Krawiec, Z., 2000. Design of composite plates under cyclic loading. Composite Structures 48 (1–3), 139–144.

Noor, A.K., Kim, Y.H., Peters, J.M., 1994. Transverse shear stresses and their sensitivity coefficients in multilayered composite panels. AIAA Journal 32, 1259–1269.

O'Donoghue, P.E., Atluri, S.N., 1986. Control of dynamic response of a continuum model of a large space structure. Computers & Structures 23, 199–209.

Rao, S.S., 1988. Combined structures and control optimization of flexible structures. Engineering Optimization 13, 1–16.

Rao, S.S., 1989. Optimum design of structures under shock and vibration environment. The Shock and Vibration Digit 21, 3–15.

Rao, S.S., Venkeyya, V.B., Khot, N.S., 1988. Optimization of actively controlled structures using goal programming techniques. International Journal for Numerical Methods in Engineering 26, 183–197.

Sadek, I.S., Sloss, J.M., Adali, S., Bruch Jr., J.C., 1993. Integrated design and control of laminated hybrid plates with dynamic response and buckling objectives. Journal of Sound and Vibration 163, 571–576.

Salama, M., Garba, J., Demesetz, L., 1988. Simultaneous optimization of controlled structures. Computational Mechanisms 3, 275–282.

Sloss, J.M., Sadek, I.S., Bruch, J.C., Adali, S., 1992. Design/control optimization of cross-ply laminates under buckling and vibration. ASCE Journal of Aerospace Engineering 5, 127–137.

Turvey, G.J., Marshall, I.H., 1995. Buckling and Postbuckling of Composite Plates. Chapman & Hall.

Wang, D.-A., Huang, Y.-M., 2002. Modal space vibration control of a beam by using the feedforward and feedback control loops. Journal of Mechanical Sciences 44, 1–19.

Yang, J.N., Soong, T.T., 1988. Recent advances in active control of civil engineering structures. Probabilistic Engineering Mechanics 3, 179–188.

Youssif, Y.G., Fares, M.E., Hafiz, M.A., 2001. Optimal control of the dynamic response of anisotropic plate with various boundary conditions. Mechanics Research Communications 28 (5), 525–534.